Wettability of Glass-Bead Surface Modified by Trimethylchlorosilane

Masayoshi Fuji,* Hiroshi Fujimori, Takashi Takei, Tohru Watanabe, and Masatoshi Chikazawa

Department of Applied Chemistry, Graduate School of Engineering, Tokyo Metropolitan University, 1-1 Minami-ohsawa, Hachioji, Tokyo, 192-0397, Japan

Received: April 24, 1998; In Final Form: October 8, 1998

The relationship between coverage of hydrophobic groups on modified glass bead surfaces and macroscopic properties such as wettability or dispersion ability has been demonstrated. The glass bead surfaces modified by trimethylsilyl (TMS) groups were obtained by the chemical reaction between trimethylchlorosilane molecules and surface silanols. The TMS coverage was estimated from carbon content by combustion gas analysis, using IR spectroscopy and the specific surface area determined by krypton adsorption. The macroscopic wettability of the samples for water was examined by floating tests and measuring contact angles. The results are summarized as follows. (1) The surface determination, employed in this study, enables one to measure small amounts of TMS groups on small-surface-area samples. (2) It was recognized from the results of the floating test and the contact angle measurement that macroscopic wettability changed markedly at the TMS coverage of about 50% of monolayer coverage. (3) The simulation and model of wetting can account for the wettability of a modified glass-bead particle surface. It was demonstrated that the wettability of material had a close relation to the bulkiness of modifier and the surface coverage on the molecular level.

Introduction

At the present stage, there are many unclear points regarding the relationships between nanoscopic properties of powder surface and macroscopic powder phenomena such as wettability or dispersion ability.[1−3] The purpose of this study is to improve the understanding of the macroscopic powder phenomena by various detailed discussions on the basis of nanoscopic physicochemical properties. If detailed information about the relationships between the macroscopic and nanoscopic properties of the powder surface are obtained, the surface will be designed to control macroscopic powder phenomena.

An index of macroscopical wetting of powder is usually determined by contact angle measurement. There are two main techniques for measuring the contact angle of powder samples. They are the sessile drop method using pellet, and the penetration method of liquids for packed powder. However, the former method can be used to measure in the case of contact angle more than 90°, while the latter can be used in the case of an angle less than 90°. Therefore the continuous assessment by one method is difficult as the particles change from hydrophilic to hydrophobic. Furthermore, the sessile drop method using pellet cannot eliminate the influence of surface roughness on the contact angle value.[4] Instead of these typical methods for measuring solid surface, there is a special technique to estimate the contact angle of powder. The relative wettability and flotability are characterized using the flotation response in a solution of progressively decreasing surface tension.[5−11] Although, the estimated contact angle using this method is indirect, the method is useful for estimating wettability of powder. For example, Fuerstenau et al. demonstrated that film flotation can be applied to homogeneous and heterogeneous particles by both experimental investigation and theoretical analysis.[12−14] The method is an excellent way to estimate contact angles for particles.

The purpose of this study is not to estimate the contact angle but to investigate the relationship between macroscopic wettability and surface structure on the atomic level. Therefore, to eliminate influences of aggregation among particles and the change of surface by the selective adsorption of solute which is used for controlling surface tension of solution on wettability, we use pure water and large particles without aggregation. Furthermore, in the case of a large particle, the contact angle can be measured directly, so we can discuss the relationship between the contact angle and flotation in detail.

In this study, the relationship between progressively increasing coverage of hydrophobic groups on a modified glass bead surface and the wettability has been demonstrated. The macroscopic wettability was examined by the contact angle measurement and floating tests. To help understanding the mechanism of wetting at the atomic level a computer simulation was performed.

Experimental Section

Materials. E-glass particles (EGB200MM and EGB201MM) were supplied by Toshiba Ballotini Co., Ltd. (Japan). These particle sizes were 0.60−0.85 and 0.71−1.00 mm, respectively. Density of the samples was 2.6 g/cm^3. The sample utilized for the present study was a mixture of EGB200MM and EGB201MM at weight ratio 1:1.62, so that the numbers of particles for both samples were equal. The particle surfaces and cross sections of the particles were observed using a scanning electron microscope (JXA-6100:JEOL Co., Ltd).

Surface Modification. The sample was pretreated to remove contamination as follows. The particles were washed with 30 wt % aqueous warm H_2O_2 for 2 h, followed by rinsing with water for 20 min, and then finally dried at 100 °C for 1 h in an

* Author to whom correspondence should be addressed. Tel/Fax: +81-426-77-2850. E-mail: fuji-masayoshi@c.metro-u.ac.jp.

10.1021/jp981983d CCC: $15.00
Published on Web 11/25/1998

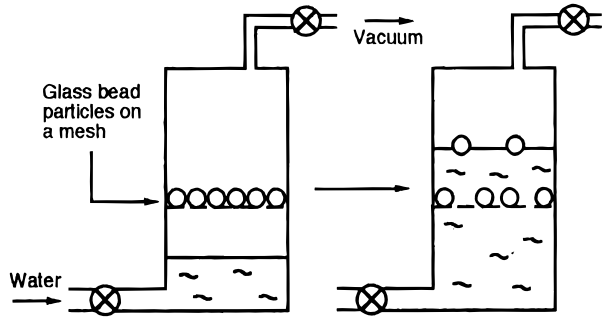

Figure 1. Schematic diagram of the apparatus for the floating test.

oven. The sample reaction was heat-treated at 450 °C for 2 h in vacuo before each silanization reaction. The silanized surfaces were obtained by the chemical reaction between trimethylchlorosilane (TMCS) molecules and surface silanol groups. TMCS was obtained from Kanto Chemical Co., Ltd. The TMCS was degassed several times using the freeze−thaw cycles method. The reaction were carried out at 300 °C in the saturated vapor pressure of TMCS for an appropriate period. Various surfaces having different amounts of trimethylsilyl groups were made. The degassing as posttreatment for removing unreacted TMCS and byproducts after modification was carried out at 450 °C for 2 h in vacuo. The surface density and coverage of TMS groups were estimated from the carbon content and the specific surface area. The carbon content was determined by combustion gas analysis. The carbon dioxide, which was generated by oxidation of TMS groups, was measured using an IR spectrometer. All the generated gas was introduced into a gas cell with known volume by condensation technique. The area of the absorbance peak, which was assigned to carbon dioxide at 2349 cm^{-1}, was converted to amount of carbon dioxide gas using a calibration curve which was predetermined for pure carbon dioxide gas. Furthermore, carbon content was estimated from the amount of carbon dioxide gas. The specific surface area was determined by krypton adsorption. The adsorption of krypton at 77 K has come into a widespread use for the determination of relatively small surface areas. The value of 0.204 nm^2 was employed as the molecular area, which is calculated from density as solid phase of krypton.

Contact Angle Measurement. The modified sessile drop technique for contact angle measurement was used. The samples were placed in a controlled-atmosphere chamber and cleaned by heat treatment at 350 °C under reduced pressure at 10^{-5} Torr before measurement. Adequate time was allowed until adsorption of water vapor was achieved prior to making the measurement. The measurement was carried out at about 25 °C for twenty samples at each coverage, and the average contact angle values was calculated. Fresh dilute water, which was confirmed from its surface tension before contact angle measurement, was used as the water for the measurement.

Floating Test. The floating test as an index of micro wettability was carried out. The procedure of the floating test was as follows. The chamber in which the sample on a mesh is installed was vacuumed before measurement for degassing air enclosed among particles (Figure 1). Then, water was slowly injected into the chamber through a stopcock, and the water surface rose gradually. Adsorption equilibrium was reached in saturated vapor pressure of water when the water surface was raised gradually and enough time was taken for the surface to arrive at bottom of the sample. When the water surface reached sufficient height, the injection of water was stopped. The floating and sinking particles were selectively removed. The upper limit of diameter for floating was defined from a crossing point of

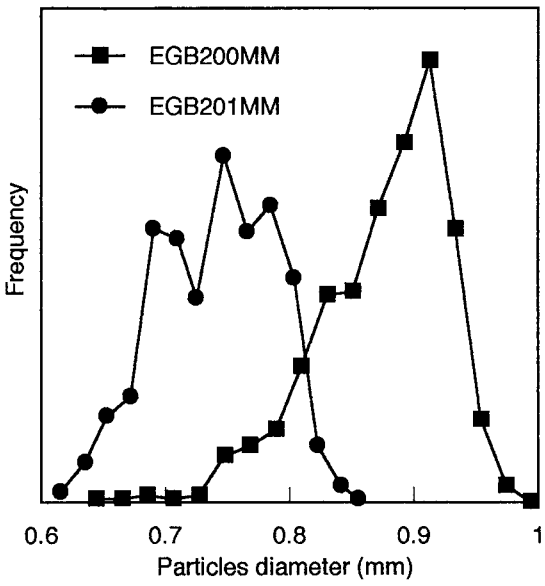

Figure 2. Particle size distributions.

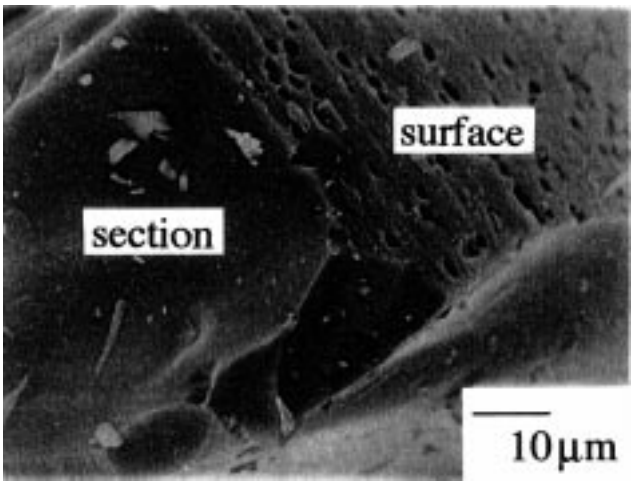

Figure 3. SEM photograph of a crushed glass bead.

these two particle size distributions. The floating rate was given by

$$F[\%] = [f/(f + t)]100 \quad (1)$$

where F is floating rate, f is the number of floating particles, and t is the number of sinking particles. The particle size distributions were estimated by statistical treatment of the bead radii which were obtained from observation for about three thousand beads.

Results and Discussion

Characterization for Glass-Bead Particles. The particle diameter distributions of EGB200MM and EGB201MM are shown in Figure 2. EGB200MM and EGB201MM were distributed mainly in the range of 0.6−0.85 and 0.75−1 mm, respectively. To examine particle-diameter dependence concerning the floating test which is shown later, an accurate measurement of distributed width of particle diameter is necessary. Therfore, the mixed sample was used at a mixing ratio of 1:1 as a number ratio of EGB200MM and EGB201MM (weight ratio, 1:1.62). SEM images of surface and cross section of the glass bead are shown in Figure 3. Concaves about 1 μm in diameter existed to a small extent on the surface. However, the

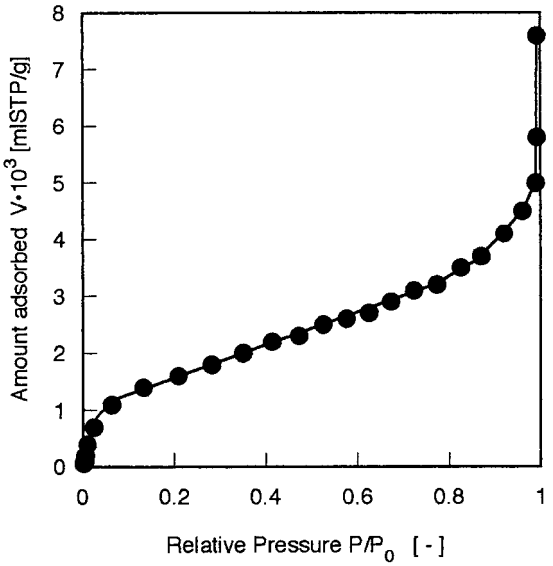

Figure 4. Adsorption isotherm of Kr for EGB200MM at 77 K.

concave on the surface of particle are shallow and the holes do not exist inside the sample.

The adsorption isotherm of Kr for EGB200MM is shown in Figure 4. This adsorption isotherm showed type II of the IUPAC classification. In general, an isotherm of type II is observed in the case of the adsorbent which has a smooth surface without micro and meso pores. The specific surface area of a mixed sample of EGB200MM and EGB201MM was 0.00657 m^2/g. When glass bead particles were assumed to be spherical, the geometrical specific surface area obtained was 0.00288 m^2/g, which was calculated by the particle diameter distribution. The former value was about 2.28 times this calculated value, and the circumference of particle was about 1.5 times the geometrical value. Moreover, the effect of surface roughness on contact angle measurement may become noticeable. However, the order of results for measurements of wettability would not be changed by the effect.

Surface Modification and Determination of Modifiers. The modification reaction was carried out between TMS molecules and surface silanols (eq 2).

$$\equiv Si-OH + (CH_3)_3SiCl \rightarrow \equiv Si-O-Si(CH_3)_3 + HCl \quad (2)$$

On the other hand, when the modified surface is burned in an oxygenic atmosphere, the oxidation would be performed as eq 3.

$$\equiv Si-O-Si(CH_3)_3 + 6O_2 \rightarrow \equiv Si-O-Si(OH)_3 + 3H_2O + 3CO_2 \quad (3)$$

Therefore, the amount of modifier will be determined by measuring the amount of generated carbon dioxide molecules. In this study, the amount of carbon dioxide was obtained by FT-IR measurement using a gas cell. The quantitative value is shown as surface density (TMS/nm^2) using the specific surface area (m^2/g) which is calculated from krypton adsorption experiments. Moreover, surface coverage (%) is calculated using the occupied area of a TMS group. There are numerous studies[15−21] about the occupied area of a TMS group. These results have a width of 0.32−0.59 nm^2. In this study, the occupied area of a modification group is employed as 0.55 nm^2 which is deduced from the following assumption.[15,19] The magnitude of the modification groups is assumed from a model

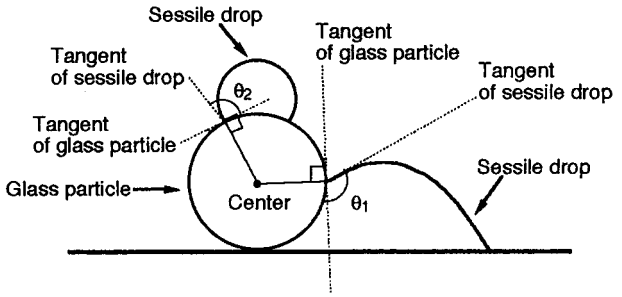

Figure 5. Contact angle measurement for spherical glass-bead particle.

TABLE 1: Results of Surface Determination

surface density [TMS groups/nm^2]	surface coverage [%] (cross-sectional area of TMS:0.55 [nm^2])
0	0
0.82	45.1
0.89	49.2
0.90	49.4
0.91	49.8
1.18	64.9
1.45	79.8
1.47	80.7
1.76	97.0

of molecular structure, and the these groups would be freely rotating. Using this value, the results of the surface determination are shown in Table 1. Samples with surface coverage about 0−100% were obtained by this modification.

Contact Angle Measurement. Among the various possibilities for the contact angle measurement method, the most generally useful contact angle for describing wetting behavior is the static advancing angle. In this experiment, the advancing angle may be obtained as θ_2 in Figure 5. Unfortunately it was not possible to measure this value in any case, since a sessile drop slipped off the top of particle. It was indicated that adhesion was weak between water and the modified surface. Therefore, θ_1 was applied as the contact angle in this study. θ_1 would be the receding contact angle, and θ_1 was smaller than θ_2 if their values are measurable. The difference is ascribed to a hysteresis effect due to chemical heterogeneity and/or solid surface roughness. The results of contact angle measurements are shown in Figure 6. The contact angle as macroscopic wettability drastically changes at TMS coverage of about 50%. This result resembles the phenomenon reported in a previous study[1] where silica powder was modified with a trimethylsilyl group and it remarkably changes at about surface coverage 40%. Such change is explained as follows. The mechanism of water vapor adsorption cannot be judged only from this experiment; however, it is expected that physisorbed water molecules cannot form a two-dimensional water layer on the modified silica surface on account of obstacles by modification groups. Such an adsorption mechanism of water vapor is confirmed from the adsorption isotherms and from comparing the adsorbed amounts with the surface adsorption sites which are reported in previous study. The difference of surface coverage between previous and present results would be attributed to differences of the initial conditions of sample surface such as surface roughness and chemical components.

Floating Test. Floating or sinking of powder materials for water depends on a force balance among gravity, buoyancy, and surface tension of water. Therefore, modification of a material is able to control the wettability of its surface. In this experiment, the floating test as an index of macro wettability was carried out. The results are shown in Figure 7 and Table 2.

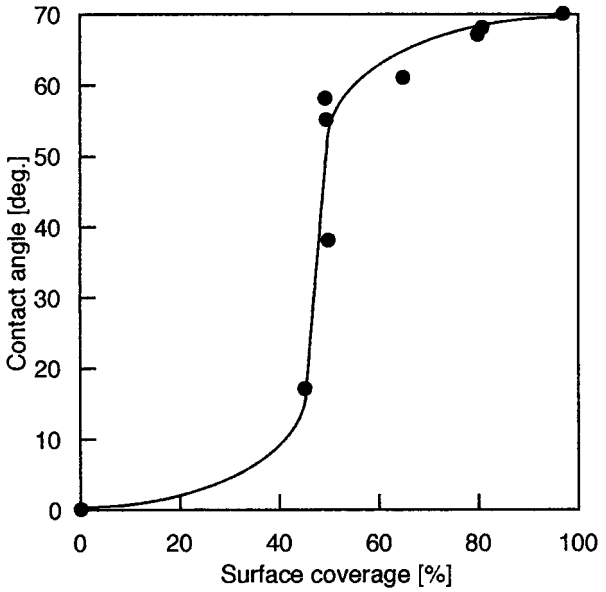

Figure 6. Relationship between surface coverage and contact angle of water on the modified glass-bead particles.

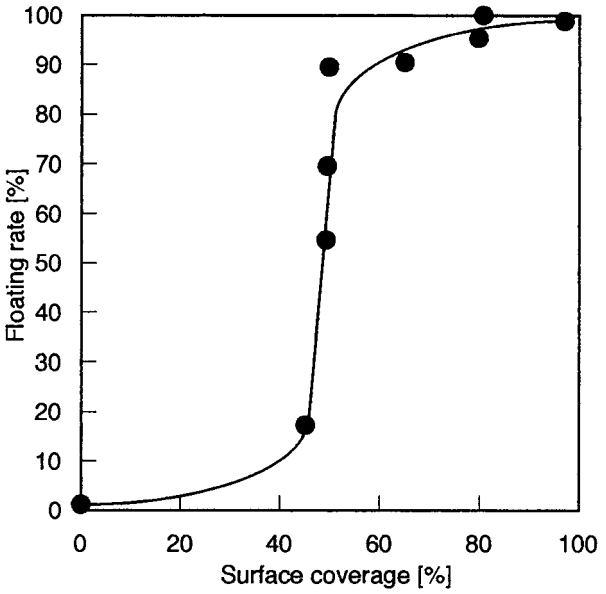

Figure 7. Relationship between surface coverage and floating rate for water of the modified glass-bead particles.

TABLE 2: Results of Floating Test

surface coverage [%]	floating rate [%]	critical particle radius [mm]
0	1	<0.6
45.1	17	0.7
49.2	55	0.9
49.4	70	0.9
49.8	89	0.9
64.9	90	1
79.8	95	1
80.7	100	>1
97.0	99	>1

The floating rate as macro wettability drastically changed at a TMS coverage of about 50%. The results of the floating test were well in accordance with the results of contact angle measurement. The relationship between modification ratio and critical particle radius to float showed a slight tendency to increase the critical radius with increasing surface coverage. It was presumed that the particle diameter distribution was narrow and skewed enough to investigate influence of a particle diameter in this experiment. As the results indicate, the change in floating or sinking occurred at similar surface coverage for every particle.

TABLE 3: Values of Physical Properties Applied for Theoretical Calculation

density of glass bead	2.6 g·cm^{-3}
density of water at 25 °C	1.0 g·cm^{-3}
surface tension of water at 25 °C	73 dyn·cm^{-1}
gravitational acceleration	9.8 m·s^{-2}

Usually, when the specific gravity of a substance is larger than that of a liquid, the substance sinks into the liquid. However, a substance will be able to float on the surface of a liquid, depending upon the magnitude of interface tension and poor wettability. In this case, the gravity for a substance balances with the resultant force of interfacial tension and buoyancy. The balance of such forces, which decides floating or sinking, are described in eq 4. The equation was introduced with the assumption that the substance is a spherical shape. The total force acting on the sample is measured as a function of the depth ratio from center of bead. The depth ratio was defined as immersion depth over the radius of bead. The forces acting on the bead during the course of the experiment are 3-fold. The first term on the left side describes the relation between the force acting at the solid/liquid/vapor interface around the perimeter of the meniscus and the contact angle formed at the interface, that is the force concerning interface tension. The second term on the left side expresses the buoyancy due to the displacement of liquid. The term on the right side represents gravity as the weight of a bead.

$$2\pi r\sqrt{1-X^2}\gamma \sin(\sin^{-1} X + \theta - \pi/2) + \pi r^3(2 + 3X + X^3)\rho_w g/3 \geq 4\pi r^3 \rho g/3 \quad (4)$$

θ: contact angle

r: radius of glass bead

d: distance between the center in a bead and water surface

X: depth ratio from center of bead ($X = d/r$)

g: gravitation acceleration

ρ: density of glass bead

ρ_w: density of water at 25 °C

γ: surface tension of water at 25 °C

Inserting the values from this experimental system as shown in Table 3, eq 4 led to eq 5.

$$\theta \geq \sin^{-1}\left\{\left(0.189 - 0.0673X + 0.224X^3\right) r^2/\sqrt{1-X^2}\right\} - \sin^{-1} X + \frac{\pi}{2} \quad (5)$$

The relationship between the contact angle and the particle radius in the range of the depth ratio $0 \leq X < 1$ is shown in Figure 9. The upper sides of the curves are the conditions of floating for each particle size. The curves have minimum values, and the contact angle values at these points are indispensable conditions for floating of particles. The contact angle as the minimum value of each particle diameter (i.e., critical diameter) is shown in Figure 10. According to the above theoretical results,

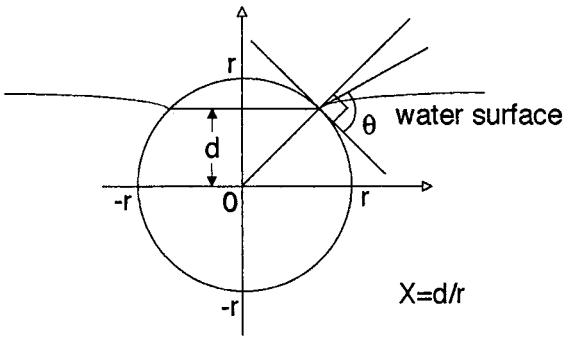

Figure 8. Model of a floating particle for theoretical calculations.

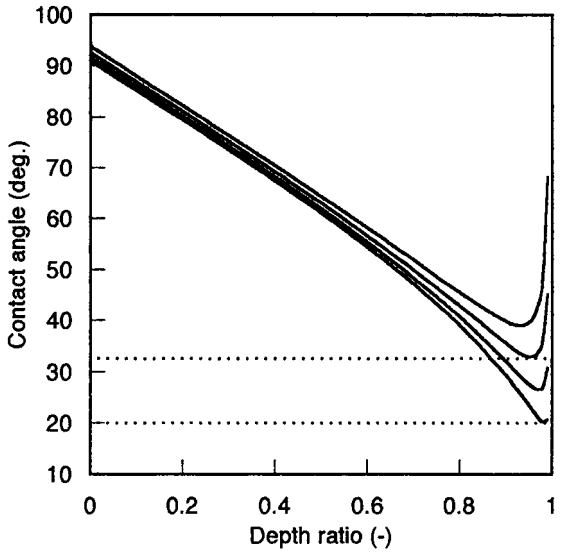

Figure 9. Floating conditions for glass particles with various radii. The curves are results for the sample radius: 0.3, 0.4, 0.5, 0.6 (mm) from bottom to top, respectively.

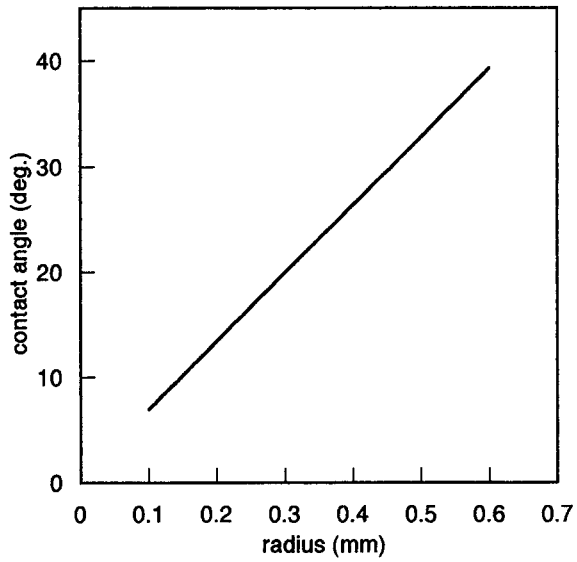

Figure 10. Floating critical contact angle for particle radius.

it is predicted that the critical particle size to float is about 20−33° for particle radius 0.3−0.5 mm. In the experimental results, half of the samples float suddenly at a surface coverage of about 50% and at contact angles of 30−40°. These experimental results were slightly larger than the results of theoretical calculations. A difference of the absolute value of both results is discussed and the cause of the difference is considered as follows.

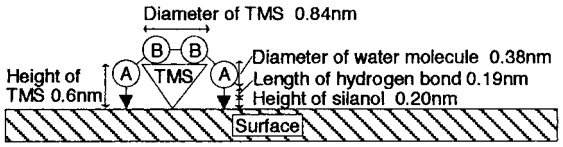

Figure 11. Cross-sectional model of a modified surface.

Surface roughness influences the contact angle. According to the theory of surface roughness of Wenzel,[4] the relationship between contact angle θ' on the surface with roughness factor R and the contact angle θ for smooth surface is shown in eq 6.

$$R = \cos\theta'/\cos\theta \tag{6}$$

In the case of contact angle below 90°, an apparent contact angle on a rough surface should be relatively small to be a true value on a smooth macroscopic surface. Therefore, macroscopic surface roughness is not a reason for the difference of the absolute value between experimental and theoretical.

The intersection of gas, liquid, and solid is not an ideal continuous straight line but nonlinear in nature. The interfacial tension is opposite a direction of gravity. Therefore, the critical contact angle to float obtained by the experiment becomes larger than the critical contact angle calculated from the theory. This consideration about the nonlinear contact line is essentially the same as the conclusions of Cassie,[22] that is, the contact angle was influenced by the heterogeneity of surface energy.[22,23] A contact angle on heterogeneous surfaces with two elements is shown in eq 7.

$$\cos\theta = f_1\cos\theta_1 + f_2\cos\theta_2 \tag{7}$$

Where f_1 and f_2 are the ratios of surfaces occupied by each element (i.e., $f_1 + f_2 = 1$). Here, the value f_2 corresponds to surface coverage of modification groups. Moreover, θ_1 and θ_2 are contact angles for homogeneous surface of each element. To calculate the critical contact angle using eq 6 the contact angle for the unmodified glass was assumed to be 0° and the contact angle for a completely modified surface is used as 70° which is the maximum value in the contact angle measurement. As a result, a contact angle for this experimental system is calculated as 48° at a surface coverage of 50%. This value is close to the experimental value (ca. 50°). Therefore, it was concluded that the effect of nonlinearity of gas, liquid, and solid interline on the contact angle was controlled by surface heterogeneity rather than by macroscopic surface roughness.

Relationship between Surface Structure and Wetting. From the examination results of wettability, drastic increases in contact angle and floating rate are observed at surface coverage of about 50%. In other words, the sample surface changes remarkably from a hydrophilic to a hydrophobic surface at surface coverage of about 50%. Moreover, it is suggested that surface structure in the molecular scale influences the wetting of the sample surface. It is considered from the theoretical model that the remarkable change of wetting corresponds to surface structure. The surface model from a sectional direction is shown in Figure 11. These models are made after reviewing literature values for the structure of water[24−28] and silanol.[29−31] The height of silanol is assumed to be 0.20 nm. This height is obtained from the assumption as follows, the distances of Si−O and O−H bonds are 0.17 and 0.10 nm, respectively, the angle of Si−O−H is 109°,[29] the hydrogen bond distance (O···H) between the water molecule and silanol is 0.19 nm. This value is estimated from the hydrogen bond distances 0.29 nm among (O···O) of water molecules and the O−H distance 0.1 nm in a water molecule.[24]

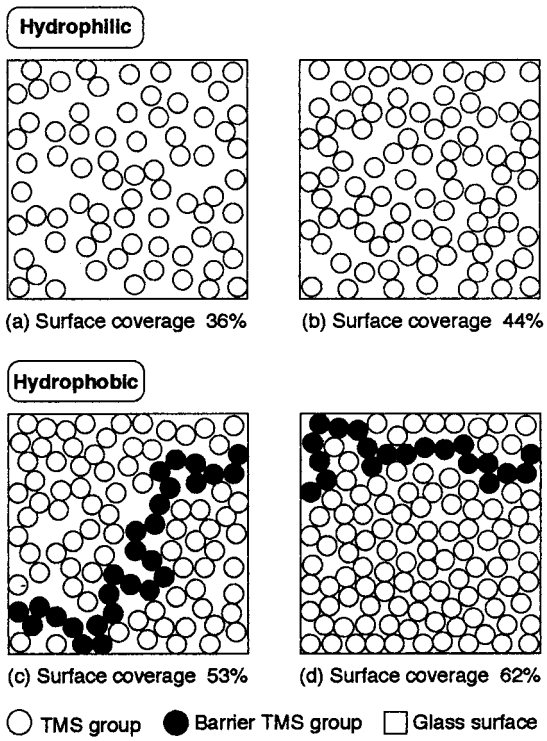

Figure 12. Typical results of graphical simulation for surface coverage.

The diameter of a water molecule was obtained as 0.38 nm, which was calculated from the cross-sectional area of 0.11 nm^2 for a water molecule. Moreover, the height of the TMS group is used as 0.60 nm, which was calculated from the liquid density of the trimethylsilane molecule and a bond distance of Si−O.[29,32] The diameter of the TMS group used was 0.84 nm which was calculated from a cross-sectional area of 0.55 nm^2.

As shown in Figure 11, the height of a silanol is about 1/3 the height of a TMS group. However, when one water molecule [Figure 11 (A)] is adsorbed on a silanol, the total height of a silanol and a water molecule becomes slightly higher than the height of TMS groups. Therefore, to form a connection with adsorbed water molecules [Figure 11 (B)] between two silanols which are separated by one TMS group, two more water molecules [Figure 11 (B)] as the intermediate substances are needed at least except for two water molecules [Figure 11 (A)] adsorbed on silanols. In other words, four water molecules [Figure 11 (A) and (B)] are necessary for a connection between the hydrophilic parts. In the case of high surface coverage, more water molecules need to connect hydrophilic parts, since the width between silanols spreads with an increase in surface density of TMS groups. However, in such a case it will be difficult to make hydrogen bonds among them. These considerations indicated the effect of the bulkiness of hydrophobic group on wettability.

The influence of surface coverage on wettability was simulated. The results are shown in Figure 12. In this simulation, modifiers were put on the substrate surface until the objective surface coverage was reached. The modification group with occupied area 0.55 nm^2 was put on the unit cell of 100 nm^2 satisfying a periodic boundary condition. A number of papers have been published concerning the reactions between chlorosilane and silica surface. In particular, Tripp et al.[33−43] reported in detail, using low-frequency infrared spectroscopy. According to their papers, the reaction condition, type, and amount of surface silanol groups influence the reaction mechanism and surface distribution of modifiers. Therefore, we should infer that the modified surface is not as simple as in this model. However, it is possible for the following reasons to discuss the effect of modifier using this model: because trimethylchlorosilane is a monofunctional reagent for surface silanol groups, the reaction mechanism would be simple in comparison with the cases of multifunctional silanes. Polymerization among silane molecules would not occur. Furthermore, it is considered that TMCS could react randomly with the surface silanol. The maximum amount of TMS group is estimated to be 1.8 nm^{-2} from cross sectional area of 0.55 nm^2 for one TMS group. This value is smaller than the average concentration of silanol groups on amorphous silica, 4.6 nm^{-2}, which was reported by Zhuravlev.[44,45]

As is shown in Figure 12, water molecules are easily adsorbed among TMS groups if the coverage is less than 53%, while the space necessary for adsorption becomes very small at coverage above 62%. Then formation of continuous a two-dimensional layer is hard since the growth of the island state of water molecules was suppressed. Moreover, the barrier line, which was formed by connecting TMS groups with each other, was observed on the simulations at 53% and 62% coverage. From this point of view, it was possible to bring the hydrophilic parts into contact with each other at about surface coverage 36% and 44%, while it was hard to interact at about surface coverage 53%. At surface coverage of about 62%, the interaction among hydrophilic parts was too difficult, for the hydrophilic parts of island state decrease.

From the above, it can be concluded that the surface coverage 44−53% is the upper limit that is capable of connection among hydrophilic parts easily with intermediate of one or two water molecules, namely, the wettability of modified surface was determined by the surface coverage and the bulkiness of modifier. This model agrees with the experimental results and the mechanism of hydrophobic for powder.

Conclusions

The results of the experiments and simulations conducted on glass bead particles are summarized as follows:

(1) The surface determination method, employed in this study, enables one to measure a small amount of TMS groups on small-surface-area samples.

(2) The results of the floating test and the contact angle measurements show that the macroscopic wettability changed markedly at TMS coverage of about 50%.

(3) The simulation and model of wetting will account for the wettability of modified glass-bead particle surface. It was demonstrated that the wettability of material had a close relation to the bulkiness of modifier and the surface coverage on the molecular level.

Acknowledgment. The author is grateful to Toshiba Ballotini Ltd. Co. for kindly providing the samples.

References and Notes

(1) Fuji, M.; Iwata, H.; Takei, T.; Watanabe, T.; Chikazawa, M. *Adv. Powder Technol.* **1997**, *8*, 320.

(2) Fuji, M.; Ueno, S.; Takei, T.; Watanabe, T.; Chikazawa, M. *J. Soc. Powder Technol. Japan* **1997**, *34*, 646.

(3) Fuji, M. *J. Surf. Sci. Soc. Jpn.* **1997**, *25*, 100.

(4) Wenzel, R. N. *J. Phys. Chem.* **1949**, *53*, 1466.

(5) Marmur A.; Chen, W.; Zografi, G. *J. Colloid Interface Sci.* **1986**, *113*, 114.

(6) Ramesh R.; Somasundaran, P. *J. Colloid Interface Sci.* **1990**, *139* 291.

(7) Mohal, B. R.; Chander, S. *Colloids Surf.* **1986**, *21*, 193.

(8) Hornsby, D. T.; Leja, J. *Colloids Surf.* **1983**, *7*, 339.

(9) Yarar, B.; Kaoma, J. *Colloids Surf.* **1984**, *11*, 429.

(10) Aveyard, R.; Binks, B. P.; Fletcher, P. D. I., Rutherford, C. E. *Colloids Surf.* **1994**, *83*, 89.
(11) Aveyard, R.; Clint, J. H. *J. Chem. Soc., Faraday Trans*. **1996**, *92*, 85
(12) Fuerstenau, D. W.; Williams M. C. *Colloids Surf.* **1987**, *22*, 87.
(13) Fuerstenau, D. W.; Diao, J.; Williams, M. C. *Colloids Surf.* **1991**, *60*, 127.
(14) Diao, J.; Fuerstenau, D. W. *Colloids Surf.* **1991**, *60*, 145.
(15) Zettlemeyeer, A. C.; Hsing, H. H. *J. Colloid Interface Sci.* **1977**, *58*, 263.
(16) Unger, K. K.; Becker, N.; Paumeliotis, P. *J. Chromatogr*. **1976**, *125*, 115.
(17) Lowen, W. K.; Broge, E. C. *J. Phys. Chem.* **1966**, *65*, 16.
(18) Sindorf, D. W.; Maclel, G. E. *J. Phys. Chem.* **1982**, *86*, 5208.
(19) Tsutsumi, K.; Takahashi, H. *Colloid Polym. Sci.* **1985**, *263*, 506.
(20) Kiseleve, A. V.; Kuznetsov, B. V.; Lanin, S. N. *J. Colloid Interface Sci.* **1979**, *69*, 148.
(21) Snyder, L. R.; Ward, J. W. *J. Phys. Chem.* **1966**, *70*, 3941.
(22) Cassie, A. D. B. *Discuss. Faraday Soc.* **1948**, *3*, 11.
(23) Israelachvili, J. N.; Gee, M. L. *Langmuir* **1989**, *5*, 288.
(24) Wall, T. T.; Horning, D. F. *J. Chem. Phys.* **1965**, *43*, 2079.
(25) Morokuma, K.; Winick, J. R. *J. Chem. Phys.* **1970**, *52*, 1301.
(26) Bene, J. D.; Popel, J. A. *Chem. Phys. Lett.* **1969**, *4*, 426.
(27) Dikerson, G. H. F. *Chem. Phys. Lett.* **1969**, *4*, 373.
(28) Hankins, D.; Moskowitz, J. W.; Stillinger, F. H. *J. Chem. Phys.* **1970**, *53*, 4544.
(29) Sauer, J.; Schroder, K. P. *Z. Phys. Chem. Leipzig* **1985**, *266*, 379.
(30) Sauer, J. *J. Phys. Chem.* **1987**, *91*, 2315.
(31) Ferrari, A. M.; Ugliengo, P.; Garrone, A. M. *J. Phys. Chem.* **1993**, *97*, 267.
(32) Takei, T.; Yamazaki, A.; Watanabe, T.; Chikazawa, M. *J. Colloid Interface Sci.* **1997**, *188*, 409.
(33) Tripp, C. P. *J. Mol. Struct.* **1997**, *408/409*, 133.
(34) Tripp, C. P.; Kazmaier, P.; Hair, M. L. *Langmuir* **1996**, *12*, 6407.
(35) Tripp, C. P.; Kazmaier, P.; Hair, M. L. *Langmuir* **1996**, *12*, 6404.
(36) Tripp, C. P.; Veregin, R. P. N.; McDougall, M. N. V.; Osmond, D *Langmuir* **1995**, *11*, 1858.
(37) Tripp, C. P.; Hair, M. L. *Langmuir* **1995**, *11*, 1215.
(38) Hair, M. L.; Tripp, C. P. *Colloids Surf.* **1995**, *105*, 95.
(39) Tripp, C. P.; Hair, M. L. *Langmuir* **1995**, *11*, 149.
(40) Tripp, C. P.; Veregin, R. P. N.; Hair, M. L. *Langmuir* **1993**, *9*, 3518.
(41) Tripp, C. P.; Hair, M. L. *J. Phys. Chem.* **1993**, *97*, 5693.
(42) Tripp, C. P.; Hair, M. L. *Langmuir* **1992**, *8*, 1120.
(43) Tripp, C. P.; Hair, M. L. *Langmuir* **1991**, *7*, 923.
(44) Zhuravlev, L. T. *Colloids Surf.* **1993**, *74*, 71.
(45) Zhuravlev, L. T. *Langmuir* **1987**, *3*, 316.